DOI: 10.1002/ejic.200501013

A New and Fast Synthesis of Nanosized $LiFePO_4$ Electrode Materials

Alvaro Caballero,[a] Manuel Cruz-Yusta,[a] Julián Morales,[a] Jesús Santos-Peña,*[a] and Enrique Rodríguez-Castellón[b]

Keywords: Copper / Lithium ion batteries / Materials science / Nanostructures / Phosphates

$LiFePO_4$ has been prepared as highly crystalline nanoparticles (approx. 80 nm in diameter) of well-defined shape by heating a mixture containing lithium acetylacetonate, iron oxalate, ammonium hydrogen phosphate and oxalic acid under argon at 550 °C for 2 h. The resulting solid contains about 6 % magnetite (Fe_3O_4) as an impurity. Despite its small particle size, this nanomaterial exhibits relatively poor electrochemical performance in lithium cells owing to its lack of electronic conductivity. Its electrochemical response contrasts with previously reported data for nano-$LiFePO_4$ materials prepared at such low temperatures. In order to overcome its lack of conductivity, the compound was treated with a copper precursor. The copper phosphate nanocomposite thus obtained exhibits improved electrochemical performance in terms of capacity and cycling life in lithium cells. Thus Cu-$LiFePO_4$-based cells deliver capacity values close to 80 mAh g^{-1} over at least 50 cycles under a C/10 regime. These values testify to the usefulness of the proposed synthetic method for preparing nanoparticulated lithium phosphate-based electrodes.
(© Wiley-VCH Verlag GmbH & Co. KGaA, 69451 Weinheim, Germany, 2006)

Introduction

Recently, a new class of cathode materials based on polyanionic compounds has aroused much interest among researchers, particularly $LiFePO_4$, which is a compound with an olivine-type structure that yields a flat voltage plateau at 3.5 V during charging and a theoretical capacity of 170 mAh g^{-1}.[1] There have been many attempts to overcome the electronic and lithium-diffusion limitations of this electrode, which impair its electrochemical performance under high-current regimes. Some authors have obtained acceptable cycling properties by coating the particles with carbon, usually by pyrolysing organic compounds during the synthesis[2–5] or by decomposing a gaseous carbon precursor onto the phosphate at 700 °C,[6,7] whereas other authors have dispersed a metal (copper or silver[8]) in the phosphate or added a conductive organic compound such as polypyrrole.[9] The intrinsic electronic conductivity can also be increased by doping the structure with ions such as Mg^{+2}, Al^{+3}, Ti^{+4} or Nb^{+5}, among others.[10,11]

The most common method for obtaining $LiFePO_4$ is a solid-state reaction involving the decomposition of various oxy salts. The reaction takes place at moderate temperatures, where the size of the as-formed phosphate particles is in the micron range.[12] Because lithium diffusion in the olivine structure is very slow (10^{-18} cm^2 s^{-1}),[3,13] some authors have noted the importance of controlling particle size.[4,12,14,15] Thus, Prosini et al.[14] have reported that chemical lithiation of nanosized anhydrous $FePO_4$ by lithium iodide and subsequent heating under an Ar/H_2 atmosphere at 550 °C produces nanoparticulated $LiFePO_4$ with very good electrochemical activity; however, this procedure requires a pristine nanomaterial. Huang et al.[4] have succeeded in limiting the size of $LiFePO_4$ by introducing oxidized carbon particles as nucleating agent. The particles obtained at 700 °C were 100–200 nm in size. Recently, Hsu et al.[15] have used a method involving the calcination of a mixture of citric acid, iron oxalate, diammonium hydrogen phosphate and lithium carbonate to obtain nanometric phosphates over the temperature range 400–900 °C. Interestingly, it was necessary to decompose the oxalates and citrate at around 700 °C in order to obtain an electroactive powder; below this temperature the organic compounds are seemingly incompletely decomposed, so the carbon coating required to ensure electronic conductivity in the phosphate is not formed. Singhal et al.[7] have precipitated a precursor by using lithium oxalate, iron hydroxide and $NH_4H_2PO_4$. Heating at 350 °C and annealing between 550 and 800 °C provided $LiFePO_4$ in particles sizes over the range 5–50 nm.

In this work, we use a method that produces nanoparticulated spinels with excellent performance in lithium ion batteries. The method involves the mechanical grinding of lithium, nickel and manganese salts in the presence of a large excess of hydrated oxalic acid[16] to obtain $LiNi_xMn_{2-x}O_4$ phases. The slurry thus obtained provides a nanomaterial upon calcination at low and moderate temperatures. We

[a] Departamento de Química Inorgánica e Ingeniería Química, Edificio Marie Curie,
Campus de Rabanales, Universidad de Córdoba, 14071 Córdoba, Spain
E-mail: iq2sanpe@uco.es
[b] Departamento de Química Inorgánica,
Universidad de Málaga, Spain

 © 2006 Wiley-VCH Verlag GmbH & Co. KGaA, Weinheim

have adapted this procedure to the phosphate phases and obtained electroactive nanosized $LiFePO_4$ at 550 °C. The material was characterised by X-ray diffraction (XRD), X-ray photoelectron spectroscopy (XPS) and transmission electron microscopy (TEM), and its electrochemical properties in lithium cells determined. The performance of the material, which was initially poorer than that of carbon-coated materials, was successfully improved by adding copper in a very low weight ratio.

Results and Discussion

Nanostructured Lithium Iron Phosphate

Lithium iron phosphate is typically prepared by heating a mixture of precursors above 500 °C. Iron(II) is usually protected from oxidation under an inert atmosphere during the thermal treatment. The introduction of carbon (or a carbon precursor such as glucose) into the system can produce iron or iron phosphides[11] during the thermal treatment by carbothermal reduction. The main difference of our method from other solid-state methods using related precursors is that it includes previous grinding and the use of a large excess of hydrated oxalic acid, two factors that seemingly have a significant effect on the results. Thus, they facilitate the formation of a highly homogeneous nanometric mixed oxalate precursor.[17] Also, the oxalic acid released during heating isolates the nanoparticles from one another, thereby hindering particle growth or agglomeration. In addition, water of hydration facilitates nucleation and growth of the reaction products. We checked the purity

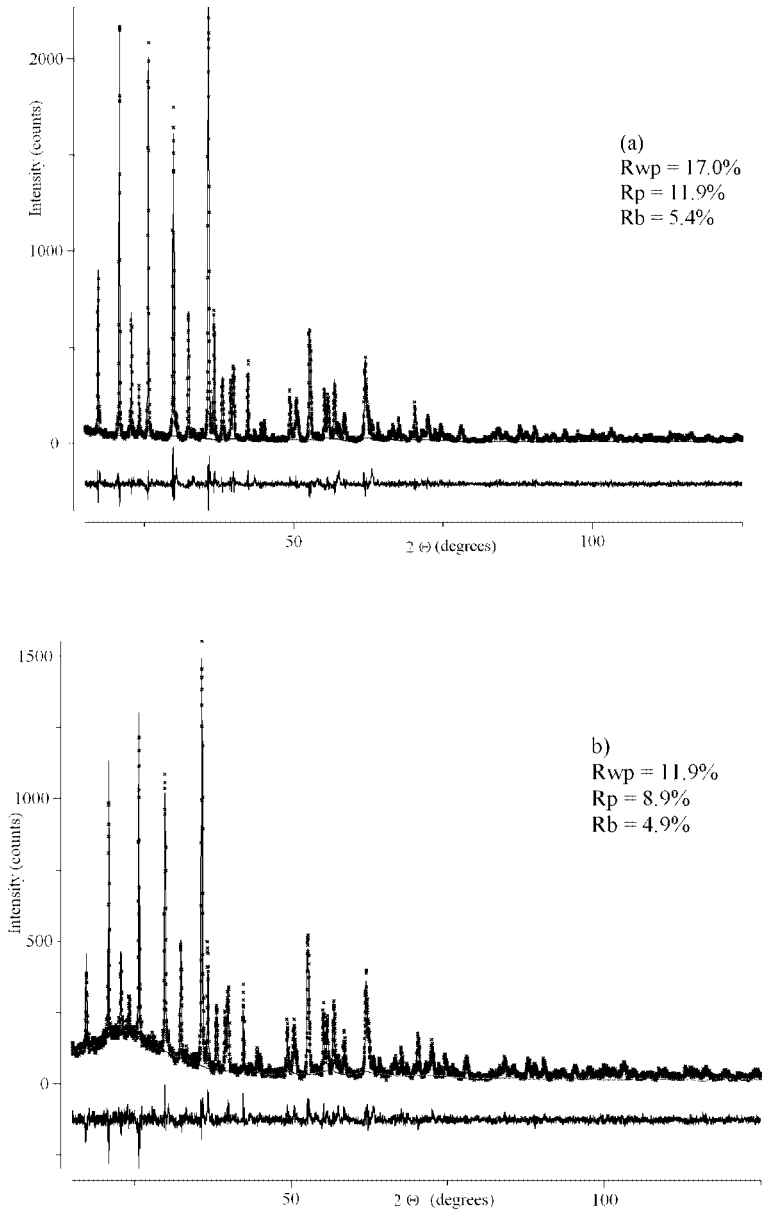

Figure 1. XRD patterns for (a) nanosized $LiFePO_4$ and (b) Cu-$LiFePO_4$ system. Experimental (dotted), calculated (line) and the difference (bottom).

 © 2006 Wiley-VCH Verlag GmbH & Co. KGaA, Weinheim

of the obtained phases by XRD (Figure 1, a). The peaks associated with the compound matched those of the orthorhombic phase (space group *Pnmb*). Rietveld refinements, performed using the GSAS software suite,[18] yielded the following cell parameter values: a = 10.298, b = 5.995 and c = 4.695 Å; $\alpha = \beta = \gamma = 90°$. The fitted parameters are included in Figure 1. There were also a few peaks at 30.35, 43.39 and 57.56° (2θ) that could not be indexed in the olivine-type structure; such peaks could be indexed in a cubic structure with a lattice constant of 8.34 Å and are consistent with either maghemite (γ-Fe_2O_3) or magnetite (Fe_3O_4). The presence of one of these phases made the sample magnetic (as checked with a magnet stick). Based on the heating temperature used, only the magnetite phase should be stable; its content as calculated from the Rietveld refinement was found to be about 6%. The magnetite may have been formed from traces of oxygen contained in the argon flow or occluded in particle pores.[12] Other authors[6] have found that $LiFePO_4$ can yield Fe_2O_3 and $Li_3Fe_2(PO_4)_3$ directly during oxidation in the air at 400 °C. Interestingly, Fe_2O_3 has been found as an impurity in a related solid-state reaction.[15] This phase seemingly appears when no citric acid − the carbon precursor used in their preparation − is present. This phenomenon was also observed by Dokko et al.,[19] who added ascorbic acid to the reaction mixture in order to remove an amorphous layer of iron oxide that appeared at 400 °C. Based on these findings, our precursors can be deemed ineffective for obtaining carbon-rich materials, as confirmed by elemental analyses.

The TEM images provided direct evidence of crystallinity in the material. The sample consists of nanoparticles (Figure 2, a) with reasonably well-defined edges and sizes below 80 nm. Figure 2 (b) shows an HRTEM image of a crystallite exhibiting structural uniformity and a lattice spacing of 0.25 nm, which corresponds to the (311) lattice planes. Note that our particles are better defined than those formed by Chimie Douce methods[14] or a related solid-state reaction at 550 °C.[15]

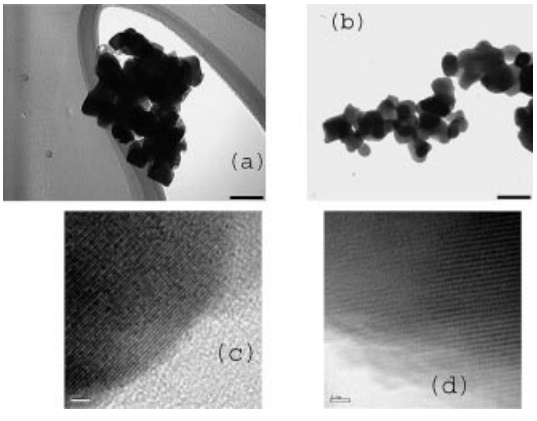

Figure 2. TEM images of (a) and (c) $LiFePO_4$; (b) and (d) Cu-$LiFePO_4$ composite. The black bar corresponds to 100 nm for the upper images and the white bar to 2 nm for the lower ones.

The oxidation states of iron and phosphorus, and the Fe/P atomic ratio, were checked by XPS. The corresponding data are shown in Table 1. The Fe/P ratio thus obtained (1.02) is consistent with the compound stoichiometry. The low intensity/background ratio of the Li 1s emission peak, which results from its low scattering coefficient towards X-rays, precluded accurate determination of its binding energy and estimation of the element content. Figure 3 (a) shows the spectrum for Fe. The shape and binding energies of the Fe 2p emission peaks are consistent with those obtained by other authors for phospholivines[20] and hinder the identification of iron oxides. Furthermore, the P 2p binding energy corresponds to the PO_4^{3-} group and rules out the presence of iron phosphide,[11] a product formed when carbothermal reduction occurs during the preparation of a phospholivine. Thus, no carbothermal reaction takes place during the calcining process.

Table 1. XPS binding energies for various atoms in the $LiFePO_4$ and Cu-$LiFePO_4$ samples.

Sample	Atom	Emission peak	Binding energy (eV)	Assignation
$LiFePO_4$	Fe	$2p_{3/2}$	711.4	Fe^{2+}
		$2p_{1/2}$	724.6	
	P	$2p$	133.7	$[PO_4]^{3-}$
	O	$1s$	531.4	$O^{=}$
Cu-$LiFePO_4$	Fe	$2p_{3/2}$	711.2	Fe^{2+}
		$2p_{1/2}$	724.4	
	P	$2p$	133.7	$[PO_4]^{3-}$
	O	$1s$	531.3	$O^{=}$
	Cu	$2p_{3/2}$	930.0	Cu^0
		$2p_{3/2}$	932.9	Cu^{I}–O
		$2p_{3/2}$	934.6	Cu^{II}–O
		$2p_{1/2}$	949.8	Cu^0
		$2p_{1/2}$	952.8	Cu^{I}–O
		$2p_{1/2}$	954.5	Cu^{II}–O

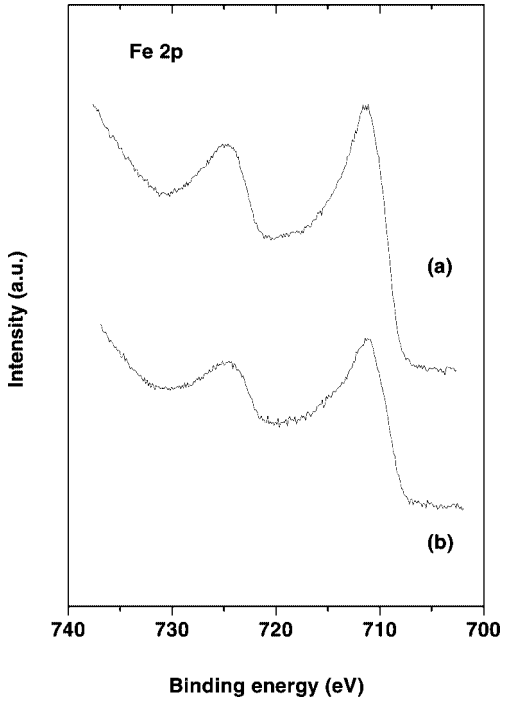

Figure 3. XPS spectrum for iron in (a) $LiFePO_4$ and (b) Cu-$LiFePO_4$.

 © 2006 Wiley-VCH Verlag GmbH & Co. KGaA, Weinheim

Figure 4 (a) shows selected potentiostatic charge/discharge curves for a cell made from nanosized $LiFePO_4$. A broad peak centred at 3.55 V was obtained in the first cycle. This oxidation peak corresponds to the extraction of lithium from the structure according to Equation (1).

$$LiFe^{II}PO_4 \rightarrow Li^+ + e^- + Fe^{III}PO_4 \quad (1)$$

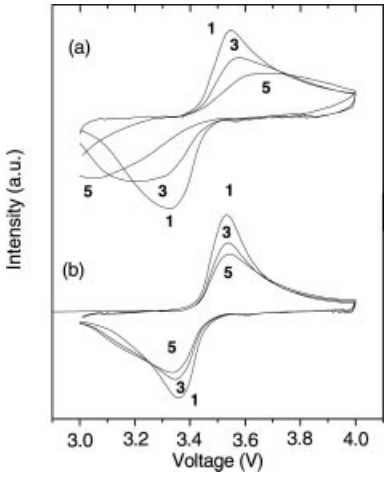

Figure 4. Voltammetric cycling of Li/$LiPF_6$(EC,DMC)/lithium iron phosphate electrodes over the 3.0–4.0 V voltage range. (a) Nanosized $LiFePO_4$, (b) Cu-$LiFePO_4$. Scan rate 5 mV/min.

The reverse reaction − the insertion of lithium into the heterosite structure − provides a broad peak at 3.33 V. The difference between both potentials, ΔE_p, is 220 mV and testifies to the kinetic limitation of these electrodes due to their high resistivity.[5,8,21] The intensity of the peaks decreased in the third cycle, which suggests that the oxidation and reduction processes are much more strongly hindered; ΔE_p rose to 360 mV. In the fifth cycle, the peaks were clearly shifted from their original positions and much broader, consistent with the decreased electrochemical activity. Figure 5 (a) shows selected galvanostatic charge/discharge cycles for the nanosized $LiFePO_4$ cell. A typical flat voltage plateau close to 3.5 V was obtained during the first charge and discharge. The first capacity was 120 mAh g^{-1}, which, however, is 50 mAh g^{-1} less than the theoretical capacity associated with the total delithiation of the phosphate. These values depart markedly from those obtained by Hsu et al.[15] for nanoparticles prepared at the same temperature, which were electrochemically inactive. Furthermore, our capacity values are higher than those found for an hydrothermally synthesised $LiFePO_4$ containing amorphous iron oxides[19] and for a nanostructured phosphate prepared by Sighal et al.[7] Note that, in the latter case, the authors used 20 wt.-% rather than 12% wt.-% carbon black to prepare the electrode mixture.

Consistent with the potentiostatic results, the capacity value was barely retained upon cycling (Figure 6) and, after five cycles, faded by 42%. This behaviour is typical of a phosphate-electrode system and illustrates the inadequate

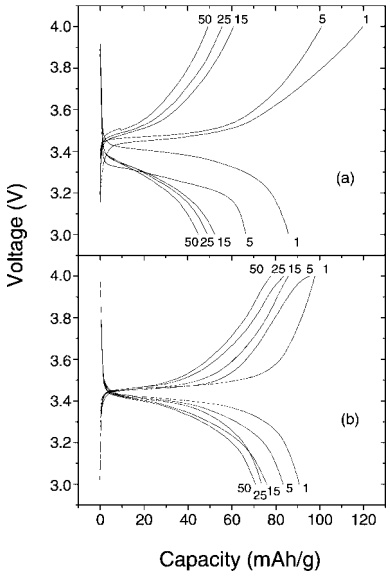

Figure 5. Galvanostatic cycles under a C/10 regime for cells with cathode based on (a) nanosized $LiFePO_4$ and (b) Cu-$LiFePO_4$.

electronic conductivity of nanoparticles. Moreover, as suggested by Yamada et al.,[12] the presence of iron oxide impurities may detract from cell performance.

Copper-Treated Lithium Iron Phosphate

As noted earlier, the nanoparticles obtained in this work, while somewhat more electroactive than other $LiFePO_4$ nanoparticles provided by more complex methods, exhibit an electrochemical response rather different from theoretical calculations and quite poor cell performance. This is widely ascribed to the lack of a carbon or phosphide network that ensures electron conduction between particles. Based on the results of Hsu et al.,[15] the electroactivity of the nanosized phosphates is determined not only by the presence of the conductive network, but also by the particle shape, which was well defined in our case. In order to improve the electrical conductivity of the electrode, we added a metal to our original material. Like Croce et al.,[8] we chose copper for this purpose on the grounds of its low toxicity and cost; however, we used a different approach that involves formation of Cu^0 in situ by chemical reduction of Cu^ICl. The reaction of this salt with $NaBH_4$ has been confirmed to yield nanoparticulated copper[22] and proceeds according to Equation (2).

$$2\,Cu^ICl + 2\,NaBH_4 \rightarrow 2\,NaCl + B_2H_6 + 2\,Cu + H_2 \quad (2)$$

Formally, the copper thus obtained should be more effectively dispersed than submicrosized commercial copper[8] and hence increase the conductivity of the Cu-$LiFePO_4$ composite.

Rietveld refinements on the XRD patterns for the new material (Figure 1, b) confirmed that the olivine-type structure was maintained during the reaction and that the cell

 © 2006 Wiley-VCH Verlag GmbH & Co. KGaA, Weinheim

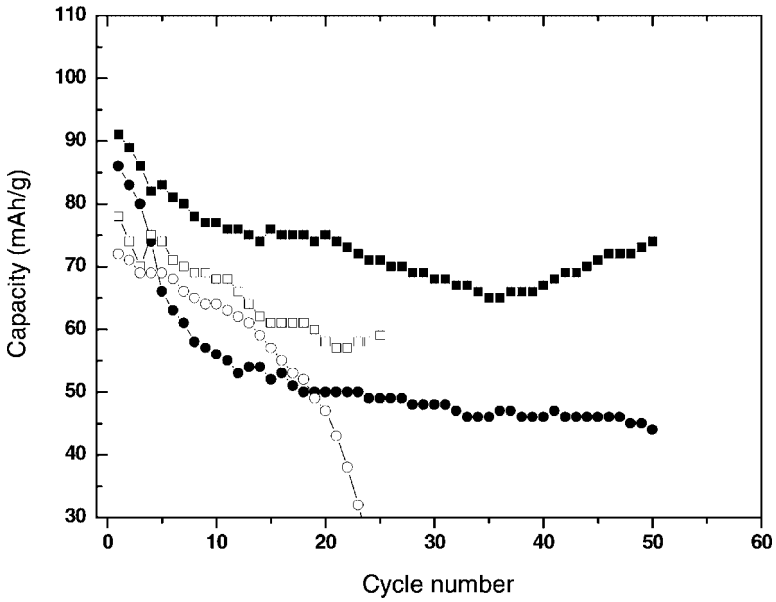

Figure 6. Variation of cell capacity as a function of the number of cycles. (●) $LiFePO_4$ under C/10, (■) Cu-$LiFePO_4$ under C/10, (○) $LiFePO_4$ under C/5 and (□) Cu-$LiFePO_4$ under C/5.

parameters were only slightly different (a = 10.302, b = 5.998, c = 4.695, $\alpha = \beta = \gamma = 90°$). No copper was detected in the XRD pattern, although iron oxide peaks were again observed. TEM images (Figure 2, b) revealed that stirring resulted in rounder particle edges and hindered the observation of well-defined particles. The crystallographic orientation of the particles was seemingly unaffected (Figure 2, d), and the d-spacing, as calculated from the fringes, was again consistent with the value for the (311) planes. No copper could be identified from TEM images. So far, all attempts at detecting isolated or agglomerated copper particles by combining microdiffraction and energy-dispersive microanalysis have failed. The diffuse diffraction peak in Cu/Li-$FePO_4$ nanocomposites should be due to a particle microstructure degradation under the stirring conditions rather than to the diffusion of Cu atoms into the phosphate framework.

The presence of copper was confirmed from XPS measurements, which also ruled out the formation of metallic iron (by reduction of Fe^{II} from the phosphate) or residual chloride. The binding-energy values obtained are listed in Table 1. The fact that the P and Fe peaks retain their positions (Figure 2, b) provides direct evidence of the stability of $LiFePO_4$ upon contact with $NaBH_4$. One unexpected finding was a complex Cu 2p profile (Figure 7) that can be resolved into the contributions of three different oxidation states (Cu^{II}, Cu^{I} and Cu^0). The presence of divalent copper is also supported by the typical shake-up observed at 940 and 943 eV. These data suggest a pronounced reactivity of Cu towards oxygen as the likely result of the nanometric size of the particles. Despite the precautions exercised to minimize contact of the composite material with the air, the element was partially oxidized, at least at a surface level. The Cu^{II}:Cu^{I}:Cu^0 atomic ratio was found to be 2:1:1. Therefore, only 1.25% by weight of the Cu-$LiFePO_4$ mixture consists of metallic copper and the improvement in conductivity should be less than expected for total conversion (5 wt.-%). This accounts for the inability to detect copper nanoparticles by XRD or from the HRTEM images.

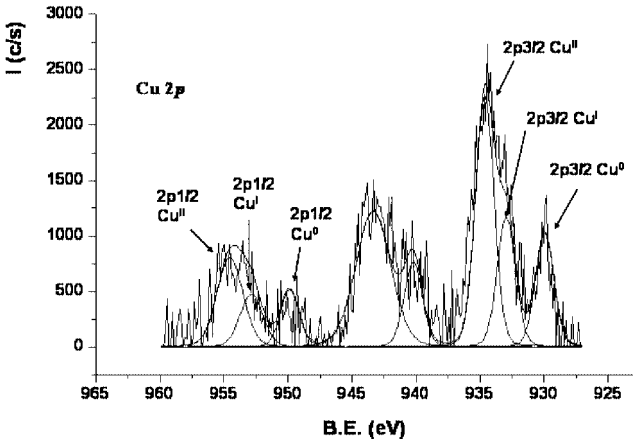

Figure 7. Cu 2p spectrum for the Cu-$LiFePO_4$ composite. Peak deconvolution is also shown.

Notwithstanding the low copper content, the favourable effect of the element on the electrochemical performance of the cell is clearly apparent. Figure 4 (b) shows the potentiostatic cycles for the cell based on the Cu-$LiFePO_4$ mixture. Now, the oxidation and reduction peaks are shaper than those for untreated $LiFePO_4$ (Figure 4, a), with this effect being stronger for the reduction peak. On further cycling, the positions of the peaks remain unchanged, even though their area decreases gradually. This suggests that electron charge-transfer is facilitated by a lower resistivity in the nanocomposite. Copper oxidation was not detected in our samples, probably because it is masked by the main reaction (the Cu potentials are 3.36–3.51 V for Cu^{2+}/Cu

 © 2006 Wiley-VCH Verlag GmbH & Co. KGaA, Weinheim

and Cu^+/Cu vs. Li^+/Li, respectively). If copper is oxidised, the as-formed Cu^I or Cu^{II} species might dissolve into the EC/DMC solvent and poison the negative electrode. Nevertheless, this plausible inconvenience seems to be negligible as the cell performance is maintained even for bigger amounts of Cu, as reported by Croce et al.[8]

Galvanostatic cycling (Figure 5, b) also provided direct evidence of the favourable effect of copper on the electrochemical properties of the electrode. In the first charge, the compound provided a flat voltage profile and a capacity of 100 mAh g^{-1}; however, 10 mAh g^{-1} was lost after discharge. The voltage plateau remained remarkably stable on cycling, but the plateau length decreased with cycling. The composite retained part of the capacity and voltage profiles over several cycles (Figure 6, b); thus, 70% of the original capacity was retained in the 50th cycle. In order to further check the performance of our composites we tested the electrodes under a faster regime, i.e. C/5. As shown in Figure 6, the faster cycling lowered the capacity for the first cycle. However, and once again, the copper composite showed a higher capacity retention (75% in capacity in the 25th cycle vs. 50% for the copper-free material). This means that the addition of Cu is insufficient to obtain high capacities under higher charge/discharge rates. The presence of iron oxides may be an important factor that hinders approach to the theoretical capacity values. We expect to be able to avoid the formation of this phase either by using alternative precursors or by modifying the thermal treatment.

Conclusion

Well-crystallised nanometric $LiFePO_4$ of uniform particle size (ca. 80 nm) was synthesised at 550 °C by using a simple method involving a homogeneous mixture of iron oxalate, diammonium hydrogen phosphate, lithium acetylacetonate and excess oxalic acid plus grinding. In contrast to the typically inactive or poorly active nanomaterials provided by alternative solid-state reactions at the same temperature, our nanomaterial is electroactive in lithium batteries. The initial charge capacity of the cell, 120 mAh·g^{-1}, was not completely recovered during the first discharge owing to the poor electronic properties of the material – no chemical treatment such as the addition of a conductor (e.g. carbon) was performed. In order to improve the cycling efficiency, we introduced copper (hypothetically in nanosized form) thoroughly mixed with the phosphate via a chemical reaction. Although copper was partially oxidized, a small fraction (less than 1.5% by weight) sufficed to increase the reversibility of the lithium extraction/insertion process by a factor close to 2 relative to the copper-free material. The capacities delivered by the Cu-$LiFePO_4$ composite in the 50th cycle were close to 80 mAh·g^{-1}. These electrochemical properties are acceptable for a nanophosphate prepared in a fast one-step method using a moderate temperature. The electroactivity of our sample appears to be determined by two main factors, namely: the nanometric size of the particles and their well-defined shape. We are currently analysing carefully the influence of both factors on the electrochemical properties of the phosphate. The proposed method can also be used to prepare other phospholivines such as $LiMnPO_4$ and $LiCoPO_4$, the electrochemical properties of which will be reported in a future paper.

Experimental Section

Lithium iron phosphate was obtained as follows: $FeC_2O_4{\cdot}2H_2O$ (1.80 g; Fluka), $(NH_4)_2HPO_4$ (1.32 g; Fluka), $LiC_5H_7O_2$ (1.60 g; Strem Chemicals), and $H_2C_2O_4{\cdot}2H_2O$ (8 g; Fluka) were ball-milled in a Retsch mill at 50 rpm for 30 min. The resulting slurry was supplied with 2 mL of ethanol and air-dried. The powder collected was subsequently calcined at 550 °C under argon for 2 h. We chose this moderate temperature in order to ensure adequate crystallinity in the compound and avoid sintering, which increases particle size. After cooling to room temperature, a brown solid, nanometric $LiFePO_4$, was obtained. For copper coating, the nanomaterial was immersed in a solution containing freshly prepared CuCl in methanol.[22] The Cu/$LiFePO_4$ weight ratio used was 5:95. Because this compound is readily oxidized, the process was carried out inside a glove box (Mbraun 150). After addition of several milligrams of $NaBH_4$ under continuous stirring the brown solid darkened. The solid was collected by filtration after 2 h of stirring and thoroughly washed with methanol. dried in an inert atmosphere and stored in tightly sealed glass containers under argon for transportation.

Transmission electron microscopy (TEM) images were obtained on a Jeol 2010 microscope operating at 200 keV. Samples were prepared in an ultrasonic bath, using hexane as dispersing agent and a grid covered with a carbon perforated film. X-ray diffraction patterns were recorded with a Siemens D5000 X-ray diffractometer, using Cu-K_α radiation and a graphite monochromator. The scan conditions for structural refinement included a 15–125° (2θ) recording range, a 0.02° step size and 8 s per step. X-ray photoelectron spectra were obtained on a Physical Electronics PHI 5700 spectrometer, using non–monochromatic Mg-K_α radiation (300 W, 15 kV, 1253.6 eV) and a multi-channel detector. Spectra were recorded in the constant pass energy mode at 29.35 eV, using a 720 μm diameter analysis area. Binding energy (BE) values were referred to the C 1s peak (284.8 eV) from the adventitious contamination layer during data processing of the XPS spectra. Recorded spectra were always fitted using Gauss–Lorentz curves in order to more accurately determine the binding energy of the different element core levels. The error in BE was estimated to be ca. ±0.1 eV. The spectra for the C 1s and Cu 2p regions were initially recorded for 10 min. Such a short acquisition time was intended to avoid the previously reported reduction of Cu^{2+} species to Cu^+ by the action of the X-ray excitation source as much as possible.[23] For recording of XPS spectra, the containers were opened in the air and the pellets, rapidly transferred to the preparation chamber of the XPS spectrometer. In this way, the exposure time of the sample to air was minimised.

Electrochemical measurements were carried out in CR2032 coin cells, using an electrode mixture consisting of active material, carbon black and Teflon in a weight ratio 85:12:3. The working electrode consisted of a stainless steel grid onto which approximately 3 mg of the mixture was pressed. The electrolyte used was 1 M $LiPF_6$ in 2:1 EC/DMC as solvent. Both the reference electrode and the counter-electrode consisted of a lithium disk. Potentiostatic cycles were carried out in a MacPile II (BioLogic) potentiostat under a regime of 10 mV/2 min. Galvanostatic discharges were performed

 © 2006 Wiley-VCH Verlag GmbH & Co. KGaA, Weinheim

on a Arbin system under a regime of C/10 (i.e. one lithium mol was transferred in 10 h) or C/5 (i.e. one lithium mol was transferred in 5 h).

Acknowledgments

The authors acknowledge financial support of the Spanish's Ministerio de Educación y Ciencia (Project MAT2002-04477-C02-02). J. S. P. is indebted to the Junta de Andalucia by the Researcher's Return Program.

[1] A. K. Padhi, K. S. Nanjundaswany, C. Masquelier, S. Okada, J. B. Goodenough, *J. Electrochem. Soc.* **1997**, *144*, 1609–1613.
[2] S. Franger, F. Le Cras, C. Bourbon, H. Rouault, *J. Power Sources* **2003**, *119–121*, 252–257.
[3] S. Franger, F. Le Cras, C. Bourbon, H. Rouault, *Electrochem. Solid-State Lett.* **2002**, *5*, A231–A233.
[4] H. Huang, S.-C. Yin, L. F. Nazar, *Electrochem. Solid-State Lett.* **2001**, *4*, A170–A172.
[5] N. Ravet, Y. Chuvinard, J. F. Magnan, S. Berver, M. Gauthier, M. Armand, *J. Power Sources* **2001**, *97–98*, 503–507.
[6] I. Belharouak, C. Johnson, K. Amine, *Electrochem. Commun.* **2005**, *7*, 983–988.
[7] A. Singhal, G. Skandan, G. Amatucci, F. Badway, N. Ye, A. Manthiram, H. Ye, J. J. Xu, *J. Power Sources* **2004**, *129*, 38–44.
[8] F. Croce, A. D'Epifanio, J. Hassoun, A. Deptula, T. Olczac, B. Scrosati, *Electrochem. Solid-State Lett.* **2002**, *5*, A47–A50.
[9] G. X. Wang, L. Yang, Y. Chen, J. Z. Wang, S. Bewlay, H. K. Liu, *Electrochim. Acta* **2005**, *50*, 4649–4654.
[10] S. Y. Chung, J. T. Bloking, Y. M. Chiang, *Nat. Mater.* **2002**, *1*, 123–128.
[11] P. Subramanya Herle, B. Ellis, N. Coombs, L. F. Nazar, *Nat. Mater.* **2004**, *3*, 147–152.
[12] A. Yamada, S. C. Chung, K. Hinokuma, *J. Electrochem. Soc.* **2001**, *148*, 224–229.
[13] V. Srinivasan, J. Newman, *J. Electrochem. Soc.* **2004**, *151*, 1517–1529.
[14] P. P. Prosini, M. Carewska, S. Scaccia, P. Wisniewski, M. Pasquali, *Electrochim. Acta* **2003**, *48*, 4205–41211.
[15] K.-F. Hsu, S.-Y. Tsay, B.-J. Hwang, *J. Mater. Chem.* **2004**, *14*, 2690–2695.
[16] A. Caballero, M. Cruz, L. Hernán, M. Melero, J. Morales, E. Rodríguez Castellón, *J. Electrochem. Soc.* **2005**, *152*, A552.
[17] X. R. Ye, D. Z. Jia, J. Q. Yu, X. Q. Xin, Z. Xue, *Adv. Mater.* **1999**, *11*, 941.
[18] A. C. Larson, R. B. Von Dreele, *Los Alamos National Lab. Rep.* No. LA-UR-86, **1994**, p. 748.
[19] K. Dokko, K. Shiraishi, K. Kanamura, *J. Electrochem. Soc.* **2005**, *152*, 2199–2202.
[20] J. Lu, Z. Tang, Z. Zhang, W. Shen, *Mater. Res. Bull.* **2005**, *40*, 2039–2046.
[21] C. R. Sides, F. Croce, V. Y. Young, C. R. Martin, B. Scrosati, *Electrochem. Solid-State Lett.* **2005**, *8*, 484–487.
[22] J. A. Haber, N. V. Gunda, W. E. Buhro, *J. Aerosol Sci.* **1998**, *29*, 637–645.
[23] E. Cano, C. L. Torres, J. M. Bastidas, *Mater. Corros.* **2001**, *52*, 667–676.

Received: November 15, 2005
Published Online: March 9, 2006

 © 2006 Wiley-VCH Verlag GmbH & Co. KGaA, Weinheim